Journal of Theoretical and Applied Mechanics, Sofia, Vol.55 (2025) pp. 263-277
GENERAL MECHANICS

COMPARATIVE ANALYSIS OF THE NUMERICAL METHODS FOR INVESTIGATING MAGNETIC MOMENT PRECESSION IN φ_0-JOSEPHSON JUNCTIONS

P. ATANASOVA[1,2*], E. DIEVA[1]

[1] *Faculty of Mathematics and Informatics, University of Plovdiv, 24 Tzar Asen, 4000 Plovdiv, Bulgaria*

[2] *Institute of Mechanics, Bulgarian Academy of Sciences, Acad. G. Bonchev Str., Bl. 4, 1113 Sofia, Bulgaria*

[Received: 25 April 2025. Accepted: 15 June 2025]

doi: https://doi.org/10.55787/jtams.25.55.3.263

ABSTRACT: The Josephson junction, a fascinating element in superconductivity, is a cornerstone of quantum computer hardware. Analyzing this object requires solving differential equations, often beyond the scope of analytical solutions. This article focuses on a model of the φ_0-Josephson junction, which describes the magnetic moment precession. A critical aspect of this investigation is addressing system stiffness, a common challenge in numerical simulations. Various numerical methods are rigorously compared to evaluate their efficiency. The study highlights the key contributions to identifying effective numerical methods for accurately solving stiff systems of the junction model and demonstrating their applicability to previously inaccessible parameter regimes. This paper presents the first use of certain methods for this model, achieving higher accuracy and effectively managing stiffness.

KEY WORDS: computational mathematics, Josephson junction, magnetic moment, numerical analysis

1 INTRODUCTION

Contemporary science and technology depend on the modeling and analysis of complex systems. These systems, often defined by spatial and temporal changes, are commonly expressed through differential equations. Numerical methods, employing various techniques and algorithms [1], provide practical solutions by approximating results that traditional mathematical methods cannot easily achieve. In this framework, the Cauchy problem for systems of ordinary differential equations (ODEs) stands as a fundamental challenge, providing a basis for examining the dynamic behavior [2]. To ensure reliable outcomes, we shall confirm that they are within the

*Corresponding author e-mail: atanasova@uni-plovdiv.bg

range of the respective method. Implicit numerical methods are particularly significant in this regard, as they excel in addressing stiff problems by offering enhanced stability and precision.

Typically, Josephson junctions consist of two superconductors separated by a thin layer of dielectric or ferromagnetic material [3]. When current flows through a Josephson junction, it generates a magnetic field. The magnetic moment in the junction arises due to the formation of currents, known as Josephson currents [4]. The transfer of superconducting pairs through a thin insulating layer generates magnetic fields and moments in the system, influencing interactions with external magnetic fields [5]. Overall, the magnetic moment is a crucial concept in physics, explaining how particles and systems interact with magnetic fields and create magnetic phenomena.

Josephson junctions also play a key role in quantum computers, where they can serve as elements for storing and processing quantum information [6]. The precession of the magnetic moment is significant in spintronics as well. One of the basic mathematical models treats the phase of the Josephson junction as a linear function of time [3]. However, this model cannot accurately incorporate certain external physical parameters. For this reason, a more complex model is considered that accounts for the phase difference and the external current [5].

Physical results related to magnetization reversal are obtained in [7] using the classic Runge-Kutta method. Due to the stiffness of the system, it was not possible to study the problem in certain parameter regions using the employed numerical method. For that reason, special implicit ones applied to the investigated model are first presented in [8]. Particularly, it is the Gauss-Legendre method with collocation points.

In this study, we apply a large quantity of methods with higher-order accuracy than the one in [8]. A comparative analysis of the numerical methods is conducted, and conclusions about their efficiency are made.

2 Problem Formulation

The primary mathematical model considers the phase difference of the Josephson junction as a linear function of time. It consists of three ODEs representing the magnetic moment spatial coordinates m_x, m_y, m_z [3]. In our work we explore a more complex model of the Josephson junction. It is modeled with a system of four ODEs, three of them represent the spatial coordinates m_x, m_y, m_z of the magnetic moment and the other one accounts for the dependency between the phase difference φ and the external current I_p [7]. A numerical research for the extended model with four ODEs is conducted in [8]. However, we present a more extensive numerical approach. It includes a comparative analysis of various implicit and explicit methods

across different conditions. In comparison with the cited paper an important difference is that we implement more efficient numerical methods. A similar approach to the one presented here for the simplest model with three ODEs is made in [9].

The extended model can be expressed as follows:

$$
\begin{aligned}
\frac{d\,m_x}{dt} &= \frac{\omega_F}{1+(\alpha\,M)^2}\,(-m_z m_y + G\,r\,m_z \sin(\varphi - r\,m_y) \\
&\quad -\alpha\left[m_x m_z^2 + G\,r\,m_x m_y \sin(\varphi - r\,m_y)\right]\big) \\
\frac{d\,m_y}{dt} &= \frac{\omega_F}{1+(\alpha\,M)^2}\left(m_x m_z - \alpha\left[m_y m_z^2 - G\,r(m_z^2+m_x^2)\sin(\varphi - r\,m_y)\right]\right) \\
\frac{d\,m_z}{dt} &= \frac{\omega_F}{1+(\alpha\,M)^2}\,(-G\,r m_x \sin(\varphi - r\,m_y) \\
&\quad -\alpha\left[G\,r\,m_y m_z \sin(\varphi - r\,m_y) - m_z(m_y^2+m_x^2)\right]\big) \\
\frac{d\,\varphi}{dt} &= \frac{1}{w} I_p(t)\sin(\varphi - r\,m_y),
\end{aligned}
\tag{1}
$$

with initial conditions $m_x(0) = 0$, $m_y(0) = 0$, $m_z(0) = 1$, $\varphi(0) = 0$, $t \geq 0$, where one of the unknown functions is the phase difference, determined by the pulse current:

$$
I_p(t) = \begin{cases} A_s & \text{if } t \in \left[t_0 - \frac{1}{2}\Delta t,\, t_0 + \frac{1}{2}\Delta t\right] \\ 0 & \text{in all other cases.} \end{cases}
$$

In addition to the change in the number of unknown functions $m_x(t), m_y(t), m_z(t)$, $\varphi(t)$, there are also changes in the parameters used, which are listed below.

Primary parameters include: ω_F – resonance frequency of the ferromagnet, α – damping parameter, G – phase difference coupling parameter, r – spin-orbit coupling parameter, M - magnetic moment norm. The added parameters are as follows: w – ratio of the characteristic to the resonance frequency, A_S – amplitude of the external current, $\Delta\,t$ – time interval of current injection, t_0 – middle of the time interval of current injection.

3 Numerical Approach

The Cauchy problem with initial conditions is a fundamental concept in the theory of differential equations [1]. To present the different numerical methods we will introduce the system in the following general form:

$$\begin{aligned} &\frac{d\vec{y}}{dx} = \vec{f}(x, \vec{y}), \\ &\vec{y}(x_0) = \vec{y}_0, \end{aligned} \tag{2}$$

where $\vec{y}$ is the unknown vector function, $\vec{f}$ is given function that defines how $\vec{y}$ changes with respect to x.

In our case $\vec{y}(t)$ is the vector function $(m_x(t),\, m_y(t),\, m_z(t), \varphi(t))^T$, $x = t$ and $\vec{f}(t, m_x(t),\, m_y(t),\, m_z(t), \varphi(t))$ is the right-hand side of (1). Cauchy initial value problems for ODEs can often be solved effectively using standard numerical methods. Sometimes the problem occurs to be stiff. The definition of stiffness is displayed below.

Definition: *(Stiff problem [10])*
A system is called stiff when, for every x and $\vec{y}$ in a certain region (for all solutions of the Cauchy problem (2)), the eigenvalues $\lambda_j, j = \overline{1,r}$ of the r-dimensional Jacobian matrix $\dfrac{\partial \vec{f}}{\partial \vec{y}}$ satisfy the following conditions:

1. $Re(\lambda_j) < 0, \quad j = \overline{1,r},$
2. $C = \max\limits_j |Re(\lambda_j)| / \min\limits_k |Re(\lambda_k)| >> 1$ – the stiffness coefficient.

The stiffness in computational mathematics manifests itself as a rapid accumulation of the error. Such problems require a specific subset of numerical methods, known for their ability to handle stiffness. For this reason, we consider standard as well as specific numerical methods to analyze the difference between their application. The methods used in this investigation are described further.

Requirements

In order to solve Cauchy problem we shall determine the values of the vector-function $\vec{y}$ at different points x numerically. Let us divide the interval $[x_0, b]$ into n equal parts with a step size of $h = \frac{b-x_0}{n}$, where $x_i = x_0 + i.h$ for $i = \overline{0,n}$.

Let us assume that the right-hand side $\vec{f}(x, \vec{y})$ of the differential equation (2) and its partial derivatives with respect to y_j, $j = \overline{1,r}$ are defined and continuous in some domain $G(x, \vec{y})$. The highest order of the necessary derivative depends on the concrete method.

3.1 Euler's method

Euler's method is presented in the following manner [11]:

$$\vec{y}_{i+1} = \vec{y}_i + h \cdot \vec{f}(x_i, \vec{y}_i), \quad i = \overline{0, n-1}.$$

The order of the local error of Euler's method is $\mathcal{O}(h^2)$, where h is the step size. The global error is of order $\mathcal{O}(h)$.

3.2 Runge-Kutta methods

Runge-Kutta methods are based on the following general formula with s intermediate coefficients $\vec{k}_\ell$, $\ell = \overline{1, s}$ [12]:

$$\vec{y}_{i+1} = \vec{y}_i + h \sum_{\ell=1}^{s} p_\ell \vec{k}_\ell,$$

where h is the step size, s is the number of intermediate steps, p_ℓ are the weight factors, and $\vec{k}_\ell$, called Runge-Kutta coefficients, are computed as follows:

$$\vec{k}_\ell = \vec{f}\left(x_i + \alpha_\ell h, \vec{y}_i + h \sum_{m=1}^{s} \beta_{\ell m} k_m\right). \tag{3}$$

The coefficients $\beta_{\ell m}$, p_ℓ, and α_ℓ are usually organized in a Butcher table [13]:

$$\begin{array}{c|cccc} \alpha_1 & \beta_{11} & \beta_{12} & \cdots & \beta_{1s} \\ \alpha_2 & \beta_{21} & \beta_{22} & \cdots & \beta_{2s} \\ \vdots & \vdots & \vdots & \ddots & \vdots \\ \alpha_s & \beta_{s1} & \beta_{s2} & \cdots & \beta_{ss} \\ \hline & p_1 & p_2 & \cdots & p_s \end{array}$$

where all the coefficients are chosen such that the local approximation error to be $\mathcal{O}(h^{s+1})$. Accordingly, the global error will be $\mathcal{O}(h^s)$.

3.2.1 Explicit Runge-Kutta methods

The explicit methods are obtained when in (3) the sum is computed with $m = \overline{1, \ell - 1}$. It means that we do not use all the coefficients $\vec{k}_\ell$, $\ell = \overline{1, s}$, but only those which are already computed.

Then the Butcher table representing the coefficients for the explicit Runge-Kutta methods has the following form:

$$\begin{array}{c|ccccc} 0 & 0 & 0 & 0 & \cdots & 0 \\ \alpha_2 & \beta_{2,1} & 0 & 0 & \cdots & 0 \\ \alpha_3 & \beta_{3,1} & \beta_{3,2} & 0 & \cdots & 0 \\ \vdots & \vdots & \vdots & \vdots & \ddots & \vdots \\ \alpha_s & \beta_{s,1} & \beta_{s,2} & \cdots & \beta_{s,s-1} & 0 \\ \hline & p_1 & p_2 & \cdots & p_{s-1} & p_s \end{array}$$

The following is a selection of explicit methods that are widely utilized in numerical methods and computational techniques [11]:

RUNGE-KUTTA METHODS OF SECOND ORDER

The Butcher tables for second oreder Runge-Kutta can be seen below:

$$\begin{array}{c|cc} 0 & 0 & 0 \\ \frac{1}{2} & \frac{1}{2} & 0 \\ \hline & 0 & 1 \end{array} \qquad \begin{array}{c|cc} 0 & 0 & 0 \\ 1 & 1 & 0 \\ \hline & \frac{1}{2} & \frac{1}{2} \end{array} \qquad \begin{array}{c|cc} 0 & 0 & 0 \\ \frac{2}{3} & \frac{2}{3} & 0 \\ \hline & \frac{1}{4} & \frac{3}{4} \end{array}$$

The order of the local error of the Runge-Kutta method with two intermediate steps is $\mathcal{O}(h^3)$, whereas the order of the global error $\mathcal{O}(h^2)$.

3.2.2 RUNGE-KUTTA METHODS OF FOURTH ORDER

The most popular formula with four intermediate coefficients can be written as follows:

$$\begin{array}{c|cccc} 0 & 0 & 0 & 0 & 0 \\ \frac{1}{2} & \frac{1}{2} & 0 & 0 & 0 \\ \frac{1}{2} & 0 & \frac{1}{2} & 0 & 0 \\ 1 & 0 & 0 & 1 & 0 \\ \hline & \frac{1}{6} & \frac{1}{3} & \frac{1}{3} & \frac{1}{6} \end{array}$$

The order of the local error of the Runge-Kutta method with four intermediate steps is $\mathcal{O}(h^5)$, whereas the order of the global error $\mathcal{O}(h^4)$.

IMPLICIT RUNGE-KUTTA METHODS

In explicit methods the new value of the solution is obtained using consequently computed Runge-Kutta coefficients $\vec{k}_\ell$. In implicit methods, however, the sum (3) includes all terms, meaning that the unknowns appear on both sides of the equations. As a result, the Runge-Kutta coefficients cannot be computed sequentially. Instead, they must be determined simultaneously by solving a system of nonlinear algebraic equations at each step. It is important to note that implicit Runge-Kutta methods have the same order for both local and global errors as explicit methods.

Gauss-Legendre methods, which have been used in this paper, are a specific subset of the implicit Runge-Kutta methods derived from the collocation at Gauss-Legendre quadrature points. This choice makes Gauss-Legendre methods capable of achieving higher order accuracy [13,14]. However, methods implemented with Gauss-Legendre coefficients are often preferred for problems requiring high accuracy and when the efficiency of the integration step is critical.

The Butcher table for Gauss-Legendre method of second order has the following form:

$$\begin{array}{c|cc} \frac{1}{2}-\frac{\sqrt{3}}{6} & \frac{1}{4} & \frac{1}{4}-\frac{\sqrt{3}}{6} \\ \frac{1}{2}+\frac{\sqrt{3}}{6} & \frac{1}{4}+\frac{\sqrt{3}}{6} & \frac{1}{4} \\ \hline & \frac{1}{2} & \frac{1}{2} \end{array}$$

The Butcher table for Gauss-Legendre method of third order can be expressed as:

$$\begin{array}{c|ccc} \frac{1}{2}-\frac{\sqrt{15}}{10} & \frac{5}{36} & \frac{2}{9}-\frac{\sqrt{15}}{15} & \frac{5}{36}-\frac{\sqrt{15}}{30} \\ \frac{1}{2} & \frac{5}{36}+\frac{\sqrt{15}}{24} & \frac{2}{9} & \frac{5}{36}-\frac{\sqrt{15}}{24} \\ \frac{1}{2}+\frac{\sqrt{15}}{10} & \frac{5}{36}+\frac{\sqrt{15}}{30} & \frac{2}{9}+\frac{\sqrt{15}}{15} & \frac{5}{36} \\ \hline & \frac{5}{18} & \frac{4}{9} & \frac{5}{18} \end{array}$$

The local error of the Gauss-Legendre method is of the order of $\mathcal{O}(h^{2s+1})$, where s is the number of the Runge-Kutta coefficients. The global error is of order $\mathcal{O}(h^{2s})$.

3.3 Adams Methods

The Adams methods are multistep numerical methods for solving ODEs, based on the interpolation of previous values of the function and its derivatives. There are two main types of Adams methods: extrapolation (predictor) [15] and interpolation (corrector) [16]. They are effective in solving large systems of differential equations, as they use information from previous steps to improve the accuracy and stability of the solution.

The interpolation method cannot work on its own. For this reason it is paired with a suitable extrapolation method. The combined Adams method, as we call it in this paper, typically applies the extrapolation method first to predict the next value. Then it is followed by the interpolation method used for correction. This approach provides a good combination of speed and stability, making it suitable for a wide range of problems.

The formula derived by Adams can be expressed as follows:

$$\Delta\vec{y}_i = h\left(\vec{y}'_i + \frac{1}{2}\Delta\vec{y}'_{i-1} + \frac{5}{12}\Delta^2\vec{y}'_{i-2} + \frac{3}{8}\Delta^3\vec{y}'_{i-3} + \dots\right),$$

where $\Delta\vec{y}_n$ is the increment in the solution at step i, $\vec{y}'_n$ represents the current derivative of the solution and $\vec{y}'_{i-1}$, $\vec{y}'_{i-2}$, $\vec{y}'_{i-3}$ are finite difference approximations of higher-order differences of the derivative values at previous steps.

3.3.1 ADAMS-BASHFORTH

In general, Adams extrapolation refers to methods that use previous derivative values to predict the future solution value. Adams-Bashforth methods are a specific case of this approach. It can be emphasized that Adams-Bashforth is a special case of Adams extrapolation, where the coefficients are chosen to maximize accuracy for a given number of previous steps.
After substituting with the finite differences $\Delta\vec{y}'_{n-1}$, $\Delta^2\vec{y}'_{n-2}$, $\Delta^3\vec{y}'_{n-3}$ accordingly we get to following term cut to derivative of the fourth previous step. The formula of fourth order is expressed as follows:

$$\vec{y}_{i+1} = \vec{y}_i + \frac{h}{24}\left(55\vec{y}'_i - 59\vec{y}'_{i-1} + 37\vec{y}'_{i-2} - 9\vec{y}'_{i-3}\right)$$

The local error of the Adams extrapolation method is of order $\mathcal{O}(h^5)$. The global error is of order $\mathcal{O}(h^4)$.

3.3.2 ADAMS-MOULTON METHOD

The Adams interpolation method uses new derivative values that are yet to be computed, which makes it more accurate but requires solving non-linear equations at each step.

The Adams-Moulton formula, cut to the third previous step, can be expressed as follows:

$$\vec{y}_{i+1} = \vec{y}_i + \frac{h}{24}\left(9\vec{y}'_{i+1} + 19\vec{y}'_i - 5\vec{y}'_{i-1} + \vec{y}'_{i-2}\right)$$

The local error of the Adams interpolation method is of order $\mathcal{O}(h^6)$, whereas the global error is of order $\mathcal{O}(h^5)$.

It must be noted that in order to use the refining Adams interpolation method it shall be combined with the extrapolation one. When combining the Adams extrapolation and Adams interpolation methods, the local error of the interpolation method typically overrides the local error of the extrapolation one.

3.4 SUMMARY AND NOTATION OF THE METHODS

Table 1 showcases all the methods used in this paper. In the first column, the names of the methods can be seen; the second column presents a notation of the methods,

which later can be seen in other tables. In the third column, the global errors of the methods are presented. The fourth column shows the main characteristics of each method.

Table 1. Notation of the methods used.

Method Name	Notation	Global Error	Characteristics
Euler	Euler	$\mathcal{O}(h)$	single-step, explicit
Runge-Kutta 2nd order	RK2	$\mathcal{O}(h^2)$	single-step, explicit, two intermediate steps
Runge-Kutta 4th order	RK4	$\mathcal{O}(h^4)$	single-step, explicit, four intermediate steps
Gauss-Legendre 2nd order	GL2	$\mathcal{O}(h^4)$	single-step, implicit, increased stability and precision, two intermediate steps
Gauss-Legendre 3rd order	GL3	$\mathcal{O}(h^6)$	single-step, implicit, increased stability and precision, three intermediate steps
Adams-Bashforth 4th order	AB4	$\mathcal{O}(h^4)$	four-step, explicit, uses 4 previous derivatives
Adams-Moulton 3rd order	AM3	$\mathcal{O}(h^5)$	three-step, implicit, uses three previous derivatives

4 Results

In order to examine the magnetic moment and its precession, the system is solved numerically, and to ensure the reliability of the results and the error value during calculations, the obtained result is verified with the norm of the magnetic moment. The global absolute error is calculated using the formula

$$A_{err} = \left| \frac{\sqrt{\sum_{i=0}^{n}(m_{x,i}^2 + m_{y,i}^2 + m_{z,i}^2)}}{n} - M \right|,$$

which takes the averaged calculated value of the magnetic moment at each point i in the considered interval and by subtracting $M = 1$ (the norm of the magnetic moment) we find the deviation from this norm.

Various programming modules have been created for visualizing the magnetic moments and precession. All program modules for solving and visualising are composed in the environment of *Wolfram Mathematica* [17].

4.1 Case 1 – non stiff

The first case we examine is under the following parameter constraints $\alpha = 0.1$, $r = 0.1$, $G = 90$, $w = 0.44$, $\omega_F = 0.44$, $t_0 = 10$, $\Delta t = 10$, $A_s = 0.45$. Let us investigate the problem up to $t = 50$. Table 2 shows the order of theoretical (T_{err}) and actual (A_{err}) errors obtained in the computation process, as well as the computational time ($CT(s)$) in seconds. The table presents a comparative analysis of various numerical methods with different step sizes $h = 0.1, 0.01, 0.001$.

Table 2. Comparison of the accuracy of results obtained with different step sizes for case 1.

Method	$h = 0.1$			$h = 0.01$			$h = 0.001$		
	T_{err}	A_{err}	$CT(s)$	T_{err}	A_{err}	$CT(s)$	T_{err}	A_{err}	$CT(s)$
Euler	10^{-1}	7.1×10^{-1}	0.06	10^{-2}	5.1×10^{-2}	0.7	10^{-3}	6.1×10^{-3}	20
RK2	10^{-2}	3.1×10^{-3}	0.1	10^{-4}	3.8×10^{-6}	1.2	10^{-6}	3.8×10^{-9}	25
RK4	10^{-4}	2.2×10^{-5}	0.2	10^{-8}	2.4×10^{-9}	2.3	10^{-12}	2.3×10^{-13}	43
GL2	10^{-4}	3.6×10^{-11}	0.8	10^{-8}	1.8×10^{-12}	6	10^{-12}	3.2×10^{-14}	60
GL3	10^{-6}	2.5×10^{-15}	2.1	10^{-12}	1.1×10^{-15}	14	10^{-18}	8.8×10^{-16}	90
AB4	10^{-4}	1.0×10^{-2}	0.1	10^{-8}	2.5×10^{-7}	2	10^{-12}	2.2×10^{-11}	45
AM3	10^{-5}	5.0×10^{-5}	0.7	10^{-10}	3.3×10^{-9}	7	10^{-15}	3.3×10^{-13}	90

The explicit Euler method exhibits the highest errors among all methods, with $A_{err} = 10^{-1}$ at $h = 0.1$ and decreasing to 10^{-3} at $h = 0.001$. However, despite its simplicity and fast computational time, its accuracy remains relatively low compared to higher-order methods. RK2 provides a noticeable improvement, reducing error order significantly, while RK4 further enhances accuracy, achieving $A_{err} = 10^{-12}$ at $h = 0.001$, making it a more reliable option for moderate computational cost.

Implicit methods, such as GL2 and GL3, offer superior accuracy at the cost of increased computation time. GL2 achieves $A_{err} = 10^{-14}$ at $h = 0.001$, while GL3 reaches an impressive accuracy of $A_{err} = 10^{-16}$, albeit requiring 90 seconds of computation time, the highest among all methods. These methods are particularly useful in problems where precision is paramount.

The Adams-based methods, AB4 and AM3, strike a balance between accuracy and computational efficiency. AB4 achieves $A_{err} = 10^{-11}$ at $h = 0.001$ with moderate computational cost, whereas AM3, being slightly more accurate, attains $A_{err} = 10^{-13}$ but demands increased computation time.

How the magnetic moments evolve over time for the parameters $\alpha = 0.1$, $r = 0.1$, $G = 90$, $w = 0.44$, $\omega_F = 0.44$, $t_0 = 10$, $\Delta t = 10$, $A_s = 0.45$ is illustrated in Fig. 1. It can be observed here that, after some oscillation in the system, the coordinate m_z changes its sign, resulting in the so-called reversal of the magnetic moment. The precession of the magnetic moment is also shown below.

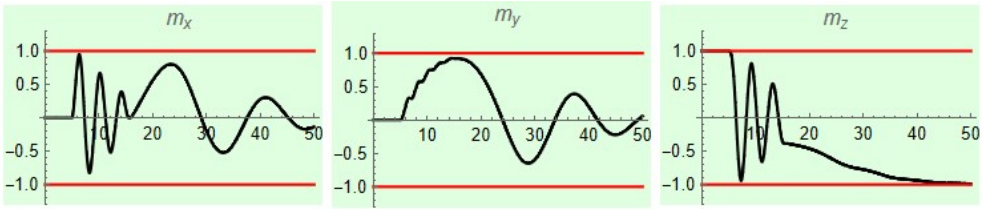

Fig. 1. Values of the spatial coordinates m_x, m_y, m_z using the fourth-order Runge-Kutta method in case 1.

Precession refers to the gradual shift or movement of the axis of a rotating object, and it often occurs in systems with angular momentum. In the context of a magnetic moment, precession involves the motion of the magnetic moment relative to an external magnetic field or a reference plane in space. The precession under the aforementioned parameters is illustrated in Fig. 2.

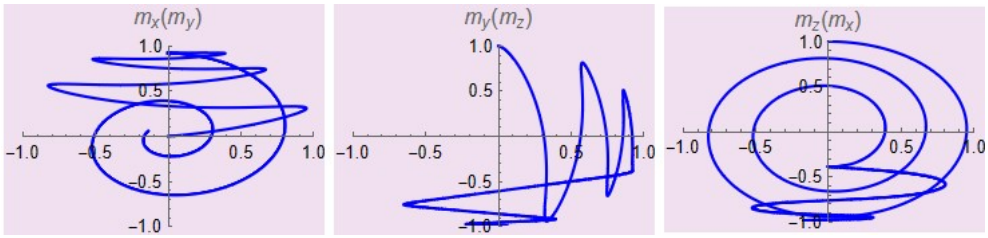

Fig. 2. Precession of the magnetic moment in case 1.

4.2 Case 2 – stiff

Another set of parameters that we consider is $\alpha = 0.3$, $r = 0.01$, $G = 60$, $w = 1$, $\omega_F = 1$, $t_0 = 10$, $\Delta t = 10$, $A_s = 0.3$. We investigate the problem up to $t = 30$. It is crucial to note that, due to numerous parameter interference in the problem,

methods that do not incorporate refinement through cyclic iterations tend to produce larger errors and may fail to achieve the anticipated order of accuracy (Table 3).

Table 3. Comparison of the accuracy of results obtained with different step sizes for case 2.

Method	$h = 0.1$			$h = 0.01$			$h = 0.001$		
	T_{err}	A_{err}	$CT(s)$	T_{err}	A_{err}	$CT(s)$	T_{err}	A_{err}	$CT(s)$
Euler	10^{-1}	—	—	10^{-2}	8×10^{-1}	0.3	10^{-3}	6×10^{-2}	6.1
RK2	10^{-2}	3.7×10^{-1}	0.06	10^{-4}	3.2×10^{-4}	0.6	10^{-6}	3.2×10^{-7}	9.3
RK4	10^{-4}	4×10^{-3}	0.1	10^{-8}	3.8×10^{-8}	1.3	10^{-12}	3.9×10^{-14}	17.3
GL2	10^{-4}	5.5×10^{-12}	1.7	10^{-8}	2.2×10^{-16}	5.9	10^{-12}	3.2×10^{-16}	50
GL3	10^{-6}	3.3×10^{-15}	8	10^{-12}	8.8×10^{-16}	16	10^{-18}	1.1×10^{-16}	90
AB4	10^{-4}	—	—	10^{-8}	4.5×10^{-6}	1.3	10^{-12}	1.1×10^{-10}	70.2
AM3	10^{-5}	1.4×10^{-2}	0.7	10^{-10}	2.4×10^{-7}	4.5	10^{-15}	1.1×10^{-11}	89.4

Simple methods, such as Euler and AB4, result in what is known as `Overflow` – an inability to continue calculations due to the limitations of the computer and the occurrence of excessively large numbers. In particular, such cases provide an opportunity to assess which methods are known for handling stiffness.

In this case, it is clearly evident that the chosen set of parameters creates a predicament for Euler's method and AB4. The explicit Euler method shows poor accuracy, with A_{err} only computes for $h = 0.01$ and $h = 0.001$. At $h = 0.01$, the actual error is 8×10^{-1}, which remains significantly high. Even at the smallest step size $h = 0.001$, A_{err} is still 6×10^{-2}, indicating relatively large accumulated errors compared to higher-order methods. However, the computation time is short, reaching only 6.1 s at $h = 0.001$.

The second-order Runge-Kutta method (RK2) improves upon Euler's accuracy, reducing A_{err} to 3.7×10^{-1} at $h = 0.1$, and further decreasing to 3.2×10^{-7} at $h = 0.001$. The computation time gradually increases from 0.06 seconds at $h = 0.1$ to 9.3 seconds at $h = 0.001$. The fourth-order Runge-Kutta method (RK4) provides even greater accuracy, with A_{err} reaching 3.9×10^{-14} for the smallest step size, while requiring 17.3 seconds of computation time.

Implicit Runge-Kutta methods (GL2 and GL3) demonstrate superior accuracy, with GL3 achieving the smallest actual error of 1.1×10^{-16} at $h = 0.001$. GL2, while slightly less accurate, remains computationally more efficient, with $A_{err} = 3.2 \times 10^{-16}$ and $CT = 50$ seconds at $h = 0.001$.

AB4 and AM3, display varied performance. AB4 does not compute for $h = 0.1$, indicating numerical instability at larger step sizes. However, for smaller step sizes, AB4 performs well, reaching $A_{err} = 1.1 \times 10^{-10}$ at $h = 0.001$, though

its computational time is considerably high at 70.2 seconds. The Adams-Moulton method (AM3) demonstrates a higher precision than AB4, reducing A_{err} to 1.1×10^{-11} for $h = 0.001$, but also requires an increased computational time of 89.4 seconds. Once again, GL2 and GL3 demonstrate the best results compared to the other methods used. These cases also open the door for exploring other, more efficient numerical methods.

The way in which magnetic moments evolve over time is illustrated in Fig. 3.

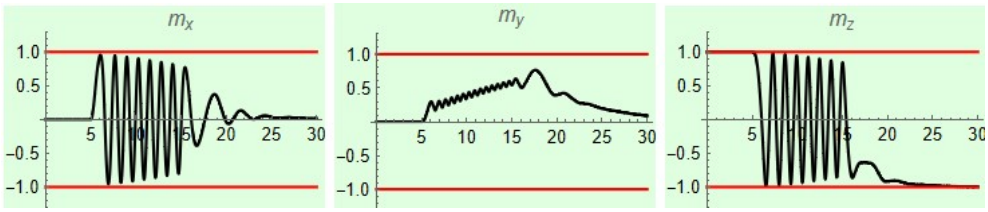

Fig. 3. Values of the spatial coordinates m_x, m_y, m_z using the fourth-order Runge-Kutta method in case 2.

The precession under the aforementioned parameters is illustrated in Fig. 4.

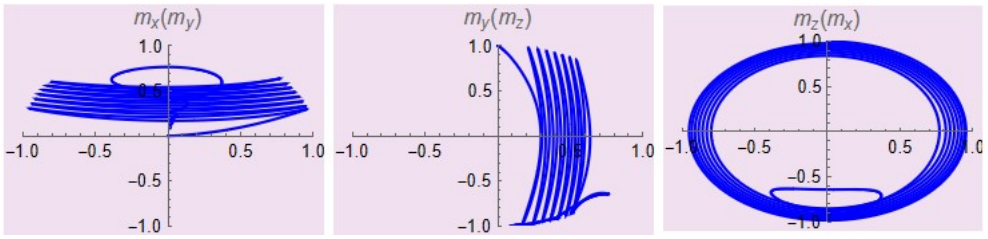

Fig. 4. Precession of the magnetic moment in case 2.

5 Conclusions

Overall, the analysis suggests that explicit methods such as Euler and RK2 offer computational efficiency but suffer from lower accuracy. RK4 provides a balanced trade-off between computational cost and precision. Implicit methods, particularly GL3, offer superior accuracy but at a significantly higher computational cost. The Adams-based methods provide a middle ground but may suffer from stability issues at larger step sizes. The selection of a numerical method must consider both the accuracy requirements and the computational feasibility of the problem.

GL3 efficiently balances precision and stability, ensuring that even in the presence of stiff components or rapid variations across different parameters, it provides reliable solutions. Moreover, despite its higher accuracy, it remains relatively time- and

CPU-efficient compared to other high-order implicit methods, making it an excellent choice for solving multiparameter problems where both performance and resource management are important. For the considered model, the best results were achieved using the GL method. This paper presents the first application of the GL3 method to the considered model, demonstrating enhanced accuracy and efficient handling of stiffness. It provides the opportunity to explore the model under parameter regimes that were previously inaccessible.

AKNOWLEDGMENTS

Pavlina Atanasova thanks the European Union-NextGenerationEU, through the National Recovery and Resilience Plan of the Republic of Bulgaria, project DUECOS BG-RRP-2.004-0001-C01.

REFERENCES

[1] R.L. BURDEN, J.D. FAIRES (2010) "Numerical analysis". 9th ed., Cengage Learning, Boston.

[2] A. BORZÌ (2020) "Modelling with ordinary differential equations: A comprehensive approach". Chapman and Hall/CRC.

[3] F. KONSCHELLE, A. BUZDIN (2009) Magnetic moment manipulation by a Josephson current. *Physical Review Letters* **102**(1) 017001.

[4] R. CITRO, C. GUARCELLO, S. PAGANO (2024) Josephson junctions, superconducting circuits, and qubit for quantum technologies. In: *New Trends and Platforms for Quantum Technologies, Lecture Notes in Physics*, vol. 1025, eds. R. Aguado, R. Citro, M. Lewenstein, M. Stern, pp. 1–55. Springer, Cham, arXiv:2405.20911 [cond-mat.supr-con].

[5] A. BUZDIN (2008) Direct coupling between magnetism and superconducting current in the Josephson φ_0-junction. *Physical Review Letters* **101** 107005.

[6] J. MARTINIS, K. OSBORNE (2004) Superconducting qubits and the physics of Josephson junctions. arXiv:cond-mat/0402415v1 [cond-mat.supr-con].

[7] YU.M. SHUKRINOV, I.R. RAHMONOV, K. SENGUPTA, A. BUZDIN (2017) Magnetization reversal by superconducting current in φ_0-Josephson junctions. *Applied Physics Letters* **110** 182407.

[8] S. PANAYOTOVA, M. BASHASHIN, E. ZEMLYANAYA, P. ATANASOVA, Y. SHUKRINOV, I. RAHMONOV (2020) Parallel Numerical Simulation of the Magnetic Moment Reversal within the φ_0-Josephson Junction Spintronic Model. *EPJ Web of Conferences* **226** 02018.

[9] E. DIEVA (2025) Numerical Analysis of the Magnetic Moment in S/F/S-Josephson Junction. *Computer Science and Interdisciplinary Research Journal* **1**(2).

[10] G. HALL, J.M. WATT (1976) "Modern Numerical Methods for Ordinary Differential Equations". Clarendon Press, Oxford; DOI:10.1007/s11075-009-9285-0.

[11] E. SULI, D. MAYERS (2003) "An Introduction to Numerical Analysis". Cambridge University Press.

[12] N.S. BAKHVALOV, N.P. ZHIDKOV, G.M. KOBELKOV (2004) "Numerical Methods". Moscow: Binom.

[13] J.C. BUTCHER (1964) Implicit Runge-Kutta Processes. *Mathematics of Computation* **18**(85) 50-64.

[14] E. HAIRER, S.P. NORSETT, G. WANNER (1993) *Solving Ordinary Differential Equations I*. Springer-Verlag, vol. 8(2), pp. 208–211, DOI:10.1007/978-3-540-78862-1

[15] S.S.S.R. ANJANEYULU, ET AL. (2024) Adams–Bashforth and Adams–Moulton methods for solving differential Riccati equations. *Computers & Mathematics with Applications* **60**(11) 3032–3045.

[16] M. ZAYERNOURI, G.E. KARNIADAKIS (2016) Fractional Adams–Bashforth/Moulton Methods: An application to the fractional Keller–Segel chemotaxis system. *Journal of Computational and Applied Mathematics* **317**(3) 1–14.

[17] WOLFRAM (accessed Feb. 20, 2022) Official website of Wolfram Mathematica. https://www.wolfram.com/mathematica/.